REINFORCED CONCRETE COLUMNS SUBJECTED TO BIAXIAL LATERAL LOAD REVERSALS

By S. Otani[I], V.W.-T. Cheung[II] and S.S. Lai[II]

SYNOPSIS

The effect of biaxial lateral loading on reinforced concrete behaviour was experimentally investigated. Loading and resulting damage in the transverse direction reduced the stiffness of a biaxially loaded column. The failure modes and overall hysteretic characteristics of a pair of identically constructed columns were similar subjected to either uniaxial or biaxial (cross displacement path) lateral load reversals. The inelastic biaxial interaction caused yielding in a direction at a load component lower than the uniaxial yield capacity. The degrading trilinear hysteresis model was confirmed to simulate major flexural behaviour of biaxially loaded reinforced concrete columns.

INTRODUCTION

The earthquake motion is not limited to one horizontal direction. Observation on damaged structures and accompanying analyses (for example,1) revealed damages caused by the response interaction due to biaxial ground motions, and triggered a series of tests on reinforced concrete columns under biaxial lateral load reversals (for example, 2 and 3). Some efforts have been made to analyze idealized structures sujected to biaxial horizontal earthquake motions (for example, 4 and 5). The basic effect of biaxial motion is to accelerate the stiffness degradation due to inelastic biaxial interaction. The stiffness degradation increases significantly the displacement response of short-period systems even under uniaxial ground motion because the displacement increases rapidly with the elongation of oscillation period. Therefore, it becomes important to study the degree of stiffness reduction due to biaxial interaction through experiment in order to provide the information to improve the reliability and accuracy of hysteretic models. The behaviour of reinforced concrete columns subjected to static biaxial lateral load reversals was studied at the University of Toronto.

EXPERIMENTAL STUDY

Specimens: The test specimens represented the portion of a first storey columns between the foundation and the inflection point. Four pairs of columns with the same overall dimensions (SP-1 through 8) were tested. The amount of lateral and longitudinal reinforcement and the strength of concrete were varied among the pairs. The reinforcement arrangement and material properties are shown in Fig. 1. Yield strengths of ties were 510, 501, 236, and 302 MPa for the four pairs. The shear resisting capacities as evaluated by the ACI Standard 318-77 (6) (with a capacity reduction factor) are 3.02, 2.74, 0.91, and 1.09 times shears corresponding to the calculated flexural capacities (with steel srain hardening) for specimen SP-1&2, SP-3&4, SP-5&6, and SP-7&8, respectively. Specimens SP-1 through 4

I Associate Professor, University of Tokyo, Japan; formerly at University of Toronto, Canada.

II Graduate Student, University of Toronto, Canada.

were designed according to the ACI Standard 318-77, while specimens SP-5 through 8 were designed to balance the flexural and shear capacities.

The loading system is schematically shown in Fig. 2. Two servo-controlled actuators were used to apply translational displacement in NS direction. A manually-controlled reversible ram was used in EW direction. Odd-numbered columns of the first three pairs were tested under uniaxial load reversals, and even-numbered specimens under biaxial load reversals (cross-shape displacement path). The last pair of specimens were subjected to simultaneous biaxial loads (square displacement path). No axial load was applied in order to simplify the experiment.

Observed Behaviour: All specimens developed flexural cracks mostly at the tie levels and diagonal cracks, both along the entire height, follwed by tensile yielding of longitudinal reinforcement and compressive crushing of concrete near the column base. X-shaped diagonal cracks appeared on all four faces of the biaxially loaded specimens, whereas diagonal cracks appeared on the two faces parallel to the loading direction in the uniaxially loaded specimens.

Specimens SP-1&2 failed by the fracture of longitudinal reinforcement at a location where a piece of metal was accidentally welded near the critical section. Later tensile tests of coupon bars showed that the fracture strain of bars with a welded piece was approximatelt 1 %, whereas that without welding was approximately 9 %. An innocent welding on reinforcement during construction can significantly reduce the ductility.

In all other specimens, crushing and spalling of concrete near the base, and splitting cracks along the longitudinal reinforcement were observed toward the end of test (Fig. 3.a and b). The behaviour was dominantly in flexure. After separation and spalling of shell concrete outside the longitudinal reinforcement cage, the core concrete was also broken into pieces due to flexural cracks, crushing of concrete, diagonal cracks, and grinding along the shear cracks. The resistance was lost through the disintegration of the core concrete and through buckling of the longitudinal reinforcement.

Effect of Lateral Reinforcement: The amount of lateral reinforcement was significantly varied between the pairs of specimens (SP-3&4 and SP-5&6), while the flexural capacities were made comparable. With heavy lateral reinforcement, both SP-3&4 developed displacement more than eleven times the calculated yield displacement, whereas specimens SP-5&6 could develop displacements approximately five times the calculated yield value. The yield displacement was evaluated by considering flexural deformation at the time when the second layer longitudinal reinforcement started to yield. A large plastic deformation of specimens SP-3&4 occurred in a concentrated region near the base, while the spalling of concrete and the disintegration of core concrete were observed in a wider region in specimen SP-5&6. It is important to provide sufficient tie reinforcement in order to increase the ductility of the critical region. At the same time, that concentrated the damage in a narrow region.

Effect of Transverse Loading: The behaviour of biaxially loaded specimens SP-4 is examined to study the effect of transverse loading. The first

yielding was observed in cycle 12 in NS direction (Fig. 4). After repeating the same amplitude displacement reversal in cycle 13, the specimen was subjected to displacement reversals in EW direction in cycles 14 through 21, displacements reaching 4.5 times the calculated yield displacement. When the specimen was subjected to a displacement reversal (cycle 22) in NS direction again at the amplitude used in cycle 13, the stiffness was expectedly reduced from that in cycle 13 as demonstrated by a dashed line. This stiffness reduction was a direct result of damage caused during loading in the transverse direction. Note that subsequent loading cycles did not show a sign of failure.

Let us study if the transverse loading will affect the ductility and load carrying capacity. Specimen SP-6 was subjected to cross-shape displacement path in NS and EW direction, while specimen SP-5 was loaded in NS direction using a displacement history obtained by combining NS and EW displacement histories of specimen SP-6. The force-deflection curves are compared in Fig. 3.c. The hysteresis loops of specimen SP-6 in NS and EW directions were combined and plotted in the same figure. The general shape of the two curves is quite similar. Failure displacements and loads were also similar in the two specimens. The damage observed near failure was comparable as shown in Fig. 3. Therefore, if simultaneous biaxial loads were not applied, the effect of transverse loading was small on ductility, load carrying capacity and damage.

Effect of Simultaneous Biaxial Loading: Specimens SP-7&8 were displaced in an approximately square shape in the horizontal plane (Figs. 5.a and 6.a), causing simultaneous loadings in the two orthogonal directions. Force-deflection relations in each direction are shown in Figs. 5.b and 6.b, and the bidirectional resistances in Fig. 7. A load stage number is used to identify the load stage in Figs 5 through 7.

In specimen SP-7, the calculated load capacity was not attained in neither NS nor EW direction, whereas the vector sum of the two components reached the calculated value at load stages 28 and 44. Although the displacement was kept almost constant in NS direction between load stages 44 and 45, the resistance dropped in NS direction due to unloading in EW direction (Fig.5). These are caused by inelastic biaxial interaction. The hysteresis loops in two successive cycles along the same displacement path are similar.

In specimen SP-8, the calculated ultimate load was exceeded at load stage 45, and nearly attained in vector magnitude at load stages 29, 46, and 47. The force-deflection curve in NS direction showed a large resistance degradation at load stages 33 and 49 compared to previous load stages 29 and 45, respectively. The resistance degradation is less when the vectorial resistances are compared.

When subjected to simultaneous biaxial loading, a column starts to yield, in a direction, at a load significantly lower than the uniaxial yield capacity due to the inelastic biaxial interaction. In other words, although a frame structure may be designed with the weak-beam-strong-column concept, column yieldings may possibly be developed during an earthquake due to the inelastic biaxial interaction.

ANALYTICAL STUDY

A reinforced concrete column under biaxial lateral load reversals can be analyzed by an elaborate finite element type model (4). However, a simple member model is normally preferred for the analysis of a structure. Takizawa and Aoyama (5) extended a one-dimensional flexural hysteretic model into a two-dimensional model, making ingenious use of plasticity theories for metal. The model performance was examined with respect to the observed behaviour of specimen SP-6. The model was subjected to the biaxial displacement history (cross-shape displacement path) observed during test SP-6. The force-deflection curves of the specimen and the model are compared in Fig. 8. The general behaviour of the specimen was simulated favourably by the model. The initial stiffness and yield point were evaluated by the flexural theory on the basis of the geometry and material properties. Cracking force level was arbitrarily chosen to be one-third the yield force level because the usage of a realistic value was not successful.

ACKNOWLEDGEMENT

The test was carried out at the Civil Engineering Structures Laboratory, University of Toronto. The study was supported by the Connaught Fund of the University of Toronto, and by the NationalResearch Council of Canada Grants.

REFERENCE

1. Okada, T., et al., "Analysis of the Hachinohe Library Damaged by 1968 Tokachi-Oki Earthquake", Proceedings, U.S.-Japan Seminar on Earthquake Engineering, Sendai, 1970, pp. 172-89.

2. Takiguchi, K., and Kokusho, S., "Hysteretic Behaviour of Reinforced Concrete Members Subjected to Biaxial Bending Moments", Proceedings, VI WCEE, New Delhi, 1977, Session 11, p. 250.

3. Maruyama, K., Ramirez, H. and Jirsa, J.O., "Behaviour of Reinforced Concrete Columns Under Biaxial Lateral Loading", Proceedings, VI ECEE, Dubrovnik, 1978, pp. 135-41.

4. Aktan, A.E., Pecknold, D.A.W. and Sozen, M.A., "Effect of Two-Dimensional Earthquake Motion on a Reinforced Concrete Column", SRS No. 399, University of Illinois, Urbana, 1973.

5. Takizawa, H. and Aoyama, H., "Biaxial Effects in Modelling Earthquake Response of R/C Structures", Journal, Earthquake Engineering and Structural Dynamics, Vol. 4, 1976, pp. 523-52.

6. American Concrete Institute, "Building Code REquirements for Reinforced Concrete", ACI Standard 318-77, Detroit, 1977.

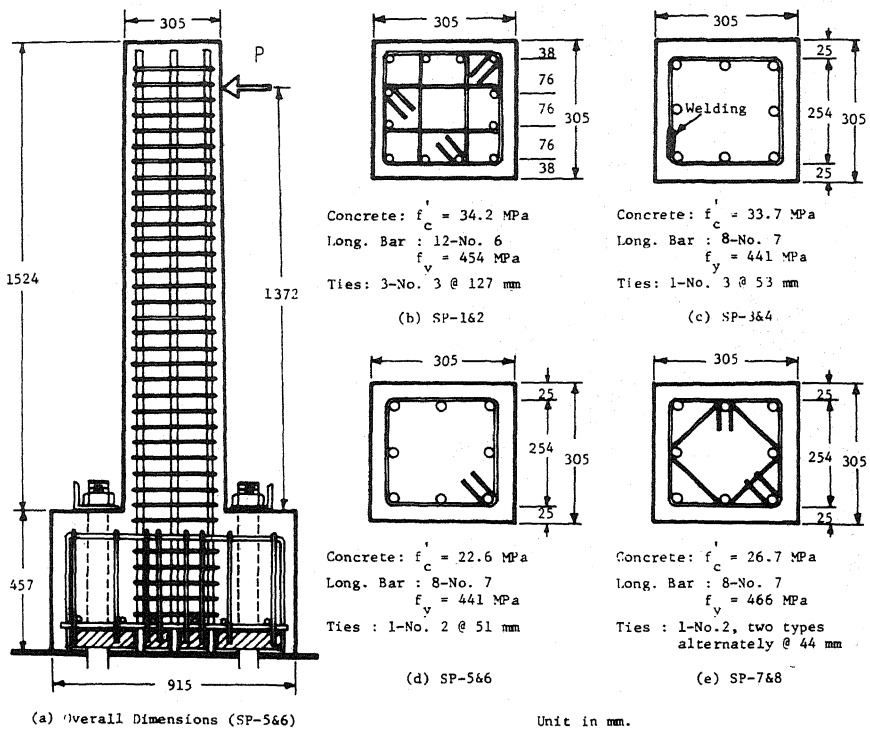

FIG. 1: Dimensions and Reinforcement of Specimens

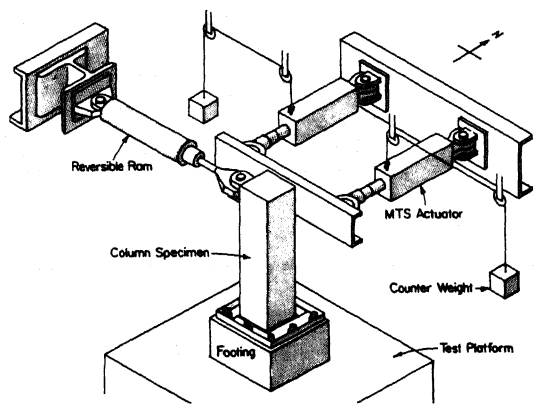

FIG. 2: Loading System for Biaxial Load Test

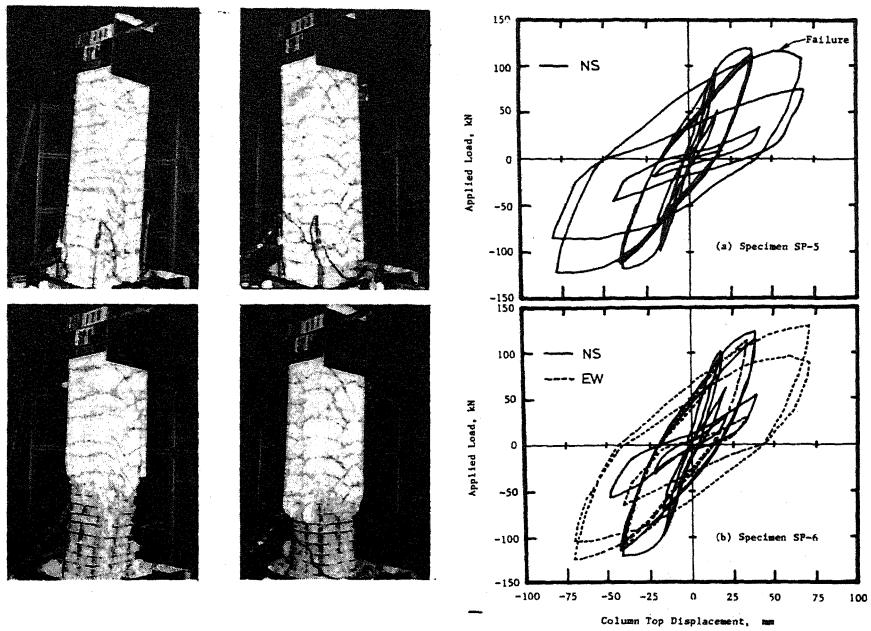

(a) SP-5 (uniaxial) (b) SP-6 (Biaxial) (c) Force-Displacement Relations

FIG. 3: Uniaxial and Biaxial (Cross Type Path) Loading

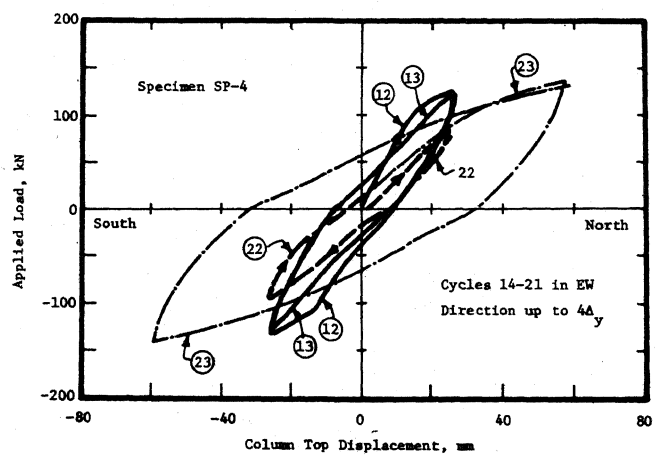

FIG. 4: Effect of Transverse Loading on Stiffness

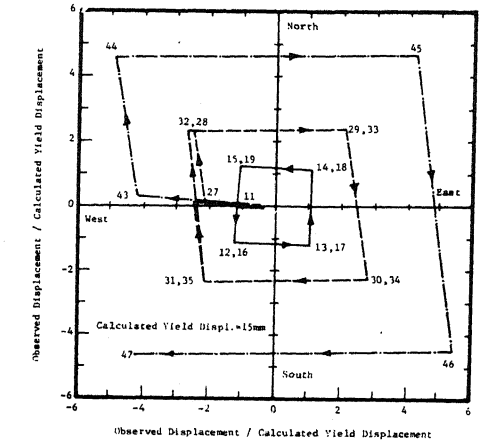

(a) Column Top Displacement Path

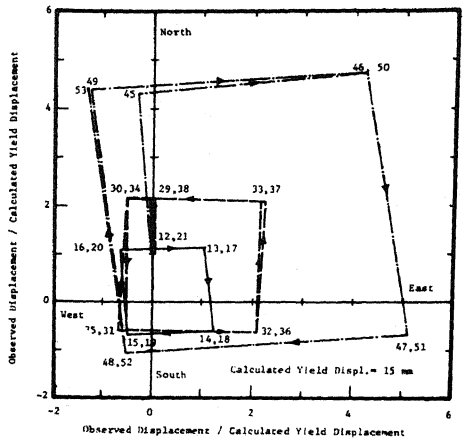

(a) Column Top Displacement Path

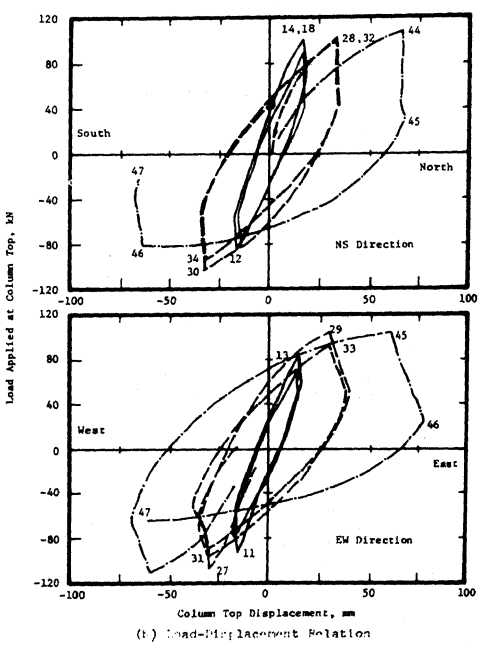

(b) Load-Displacement Relation

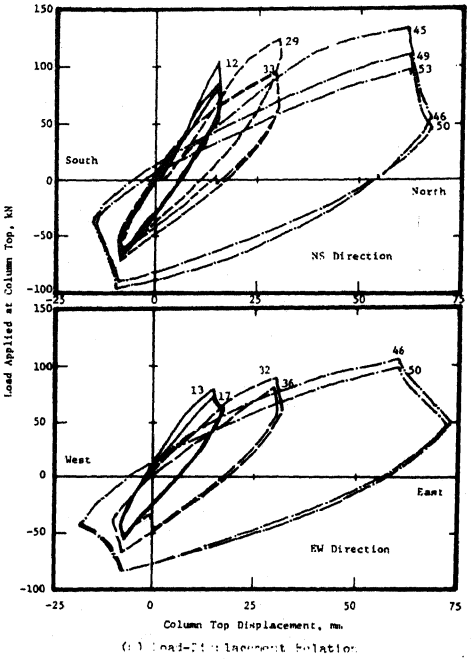

(b) Load-Displacement Relation

FIG. 5: Biaxial Specimen SP-7

FIG. 6: Biaxial Specimen SP-8

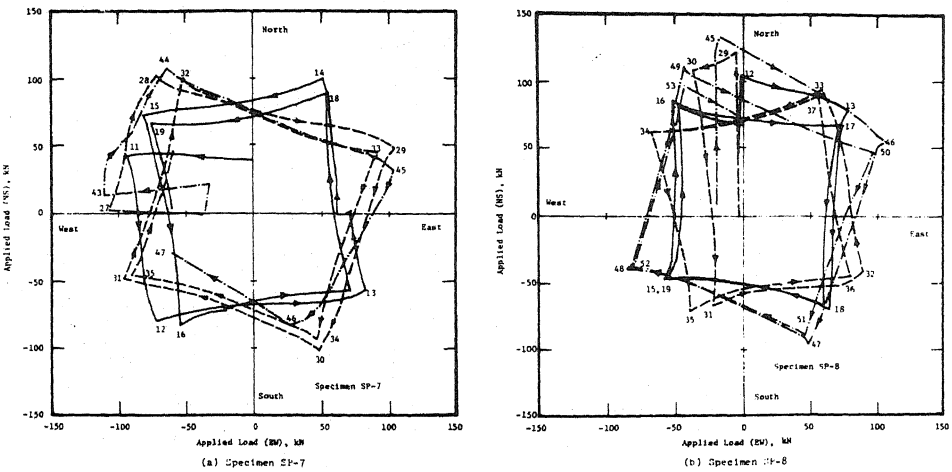

FIG. 7: Bidirectional Resistances of Biaxial Columns

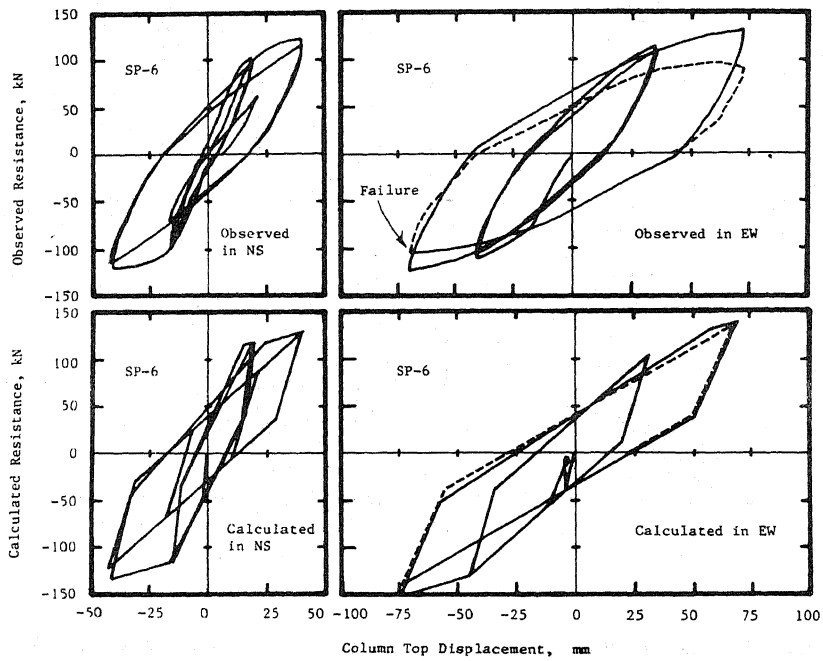

FIG. 8: Observed and Calculated (Takizawa Model) Response